The Plant Cell, Vol. 7, 271–285, March 1995 © 1995 American Society of Plant Physiologists

Specific Expression in Reproductive Tissues and Fate of a Mitochondrial Sterility-Associated Protein in Cytoplasmic Male-Sterile Bean

Andre R. Abad, Brian J. Mehrtens, and Sally A. Mackenzie[1]

Department of Agronomy, Purdue University, West Lafayette, Indiana 47907-1150

In common bean, cytoplasmic male sterility has been associated with a unique sequence found in the mitochondrial genome, designated *pvs* (for *Phaseolus vulgaris* sterility sequence). Within the *pvs* sequence, two open reading frames are encoded, ORF98 and ORF239. We have raised rabbit polyclonal antibodies against Pvs-ORF239 to evaluate the role of this putative male sterility–associated protein. Histological investigation of pollen development revealed that in the male-sterile bean line, callose deposition was abnormal and microspores remained as tetrads as previously reported. Pvs-ORF239 was found to be localized within the reproductive tissues of the male-sterile bean line, in contrast to all other cytoplasmic male sterility systems studied to date. This protein was associated with mitochondria, the callose layer, and developing primary cell walls during microsporogenesis. Expression of *pvs-orf239* was not detected in fertile plants containing restorer gene *Fr2*. These observations, together with previous reports, suggest that nuclear restorer gene *Fr2* interferes with expression of the *pvs* region post-transcriptionally.

INTRODUCTION

In higher plants, the maternally inherited phenomenon of cytoplasmic male sterility (CMS) results in the inability to produce or shed viable pollen (Hanson and Conde, 1985). CMS-associated abortion of the meiocytes has involved a number of different morphological processes, including premature dissolution of the callose surrounding the tetrad (Izhar and Frankel, 1971; Warmke and Overman, 1972; Horner, 1977) and premature autolysis of the tapetum layer (Horner and Roger, 1974; Warmke and Lee, 1977; Holford et al., 1991). In most cases of CMS, pollen sterility is associated with abnormal mitochondrial function in the sporophytic (maternal) tissue. In a limited number of examples, however, the mitochondrial abnormality predominantly affects development of the gametophytic (1N) stage (Warmke and Lee, 1977; Albertsen and Palmer, 1979; Johns et al., 1992).

In most CMS systems, abnormal development of the male reproductive tissues is correlated with modifications of the mitochondrial genome. These include aberrant recombination events, insertions, and deletions that result in unusual open reading frames (ORFs; Dewey et al., 1986; Young and Hanson, 1987; Kohler et al., 1991; Laver et al., 1991; Singh and Brown, 1991; Johns et al., 1992; Krishnasamy and Makaroff, 1993). It has been postulated that the pollen sterility phenotype is a consequence of mitochondrial dysfunction. In most cases in which the CMS system has been investigated, the mitochondrial lesion apparently affects only male reproductive development, whereas the remainder of the plant displays no phenotypic changes.

In several plant CMS systems, unique mitochondrial DNA sequences associated with sterility were shown to be transcribed and translated into proteins. In cytoplasmic male-sterile petunia, a mitochondrial sequence derived by intragenic recombination is translated into a 25-kD peptide (Nivison and Hanson, 1989). Similarly, unusual mitochondrial proteins associated with the CMS phenotype have been identified in CMS-T maize (Dewey et al., 1987; Wise et al., 1987; Hack et al., 1991) and in cytoplasmic male-sterile sunflower (Horn et al., 1991; Laver et al., 1991; Moneger et al., 1994). The most striking feature of the mitochondrial sterility-associated gene products identified to date is that they appear to be expressed in all plant tissues. Consequently, a clear association between their expression and the pollen sterility phenotype has not yet emerged.

In common bean, the CMS phenotype is associated with the presence of a unique 3.7-kb sequence, designated *pvs* (for *Phaseolus vulgaris* sterility), in the mitochondrial genome of the common bean line CMS-Sprite (Chase and Ortega, 1992; Johns et al., 1992). Restoration to fertility in bean can be accomplished by introduction of the nuclear restorer gene *Fr* (Mackenzie and Bassett, 1987) or by spontaneous cytoplasmic reversion. Both of these events involve the apparently identical loss of the region of the mitochondrial genome encompassing *pvs* (Mackenzie and Chase, 1990; Johns et al., 1992; Janska and Mackenzie, 1993). Within the *pvs* region,

[1] To whom correspondence should be addressed.

at least two ORFs have been identified, *orf98* and *orf239*, which are predicted to encode peptides of 10.9 and 26.7 kD, respectively (Chase and Ortega, 1992; Johns et al., 1992).

A second nuclear fertility restoration system has been identified in cytoplasmic male-sterile bean. In this case, restoration of pollen fertility is achieved by a single nuclear gene, *Fr2*. Restoration to fertility by *Fr2* does not involve loss of the *pvs* sequence from the mitochondrial genome (Mackenzie, 1991); rather, this nuclear gene seems to influence expression of the *pvs* sequence to restore normal pollen development. Recent evidence indicates that transcription of the *pvs* region occurs in CMS-Sprite and fertile line GO8063, which contains the restorer gene *Fr2*. A complex pattern of transcripts from within the *pvs* region (7.0, 6.8, 4.7, 3.3, and 2.8 kb) is present in young seedling (Mackenzie and Chase, 1990) and floral bud (Chase, 1994) tissues of both lines in the sense orientation to *pvs-orf98* and *pvs-orf239*. Consequently, it does not appear that the restorer gene *Fr2* directly influences transcription of this region.

In this study, we raised polyclonal antibodies against the putative protein encoded by *pvs-orf239*. This sequence was selected because it is the largest ORF encoded within *pvs*, and its predicted product contains a hydrophobic N terminus commonly found in membrane-bound proteins. We used anti–Pvs-ORF239 antibodies to investigate the pattern of expression of this unique mitochondrial sequence during development in cytoplasmic male-sterile common bean and to evaluate the effect of the restorer gene *Fr2* on expression of this sterility-associated sequence. The plant materials available for this study included CMS-Sprite, which contains the mitochondrial *pvs* sequence but no fertility restorer genes, WPR-3, a spontaneous fertile cytoplasmic revertant isonuclear to CMS-Sprite but lacking *pvs*, and the fertile restorer line GO8063, which contains *pvs* as well as the fertility restorer gene *Fr2*. In contrast to all other CMS systems investigated to date, we found the Pvs-ORF239 protein localized in pollen mother cells and subsequent microspores of CMS-Sprite anthers. Expression of this sequence was not, however, detected in these tissues in a fertile line containing *Fr2* or in the revertant. Localization of the Pvs-ORF239 product was also detected within the ovule tissues of the CMS-Sprite bean line.

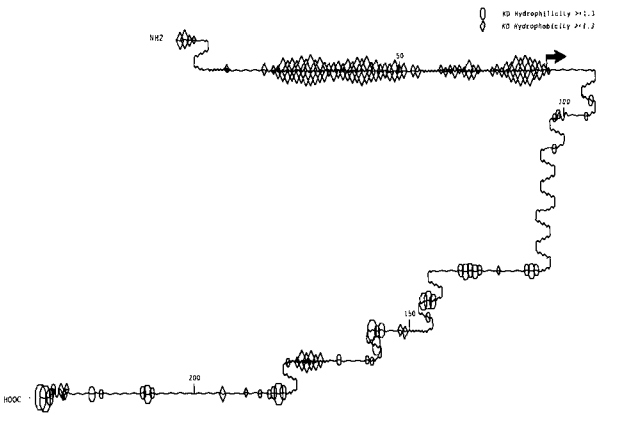

Figure 1. Pvs-ORF239 Predicted Secondary Structure.

Chou and Fasman (1978) prediction of the secondary structure and hydrophobicity characteristics of Pvs-ORF239 (Devereux et al., 1984) is shown. Helices are represented by a sine wave, β-sheets by a sharp sawtooth wave, turns by a 180° turn, and coil by a dull sawtooth wave. Hydrophilicity (threshold 1.3) is superimposed on the plot. The arrow indicates the N terminus of the truncated Pvs-ORF239 protein used as the antigen for antibody production.

RESULTS

Development of Polyclonal Antibodies against Pvs-ORF239

The expression vector pMALc used in the experiment allowed development of an in-frame fusion between the *orf239* insert and the maltose binding protein (*MBP*) gene contained 5′ to the polylinker cloning site. Because the full-length *orf239* sequence was unstable in *Escherichia coli* (data not shown), it became necessary to remove the first 82 amino acids from Pvs-ORF239. Figure 1 shows how this eliminated the hydrophobic domain to permit expression of the fusion protein. Rabbit polyclonal antibodies were raised against the intact fusion protein containing the truncated form of the Pvs-ORF239 protein. These antibodies were used in protein gel blot analysis to establish whether cross-reactivity with the truncated form of the protein was observed.

Figure 2 demonstrates that the polyclonal antibodies (referred to as anti–Pvs-ORF239) recognized the uncleaved fusion protein, MBP, and the truncated Pvs-ORF239 protein. Due to the availability of anti-MBP antibodies, the anti–Pvs-ORF239 polyclonal antibody was not affinity purified. Instead, the anti-MBP antibodies were used as a control for the specific labeling by anti–Pvs-ORF239. The observed Pvs-ORF239 cleavage product migrated at a molecular mass of 17.5 kD. The expected molecular mass of the truncated Pvs-ORF239, based on sequence, was estimated to be 17 kD. The mixture of cleaved and uncleaved fusion protein served as a positive control in all protein gel blot analyses. The truncated Pvs-ORF239 protein was purified and used as a positive control in subsequent ELISA analysis.

Test for Expression of Pvs-ORF239

The anti–Pvs-ORF239 rabbit polyclonal antibodies, characterized by gel blot analysis to cross-react with truncated Pvs-ORF239 (Figure 2), were used in ELISA experiments to test for the presence of Pvs-ORF239 protein in plant tissues. The titer of the Pvs-ORF239 antibodies was evaluated by absorbing into the ELISA microtiter plate wells 5 ng of the purified truncated Pvs-ORF239 dissolved in coating buffer with 95 ng of BSA and incubating with a serial dilution of the antibodies. Incubation of the ELISA microtiter plate for 1 hr

gave a reading of 0.974 with a 1/2500 dilution of the serum. In all subsequent analyses, wells containing 1, 3, 5, and 10 ng of purified truncated Pvs-ORF239 were included in all of the ELISA experiments. The limit of detection by the polyclonal antibodies was generally ~1 ng of Pvs-ORF239, giving an absorbance reading of 0.2 above background.

To test for the presence of Pvs-ORF239 protein in plant tissues, dilution of the antibodies was 1/1700. Mitochondrial and total protein preparations from roots, young etiolated seedlings, leaves and fractionated total protein from anthers of CMS-Sprite (*pvs*$^+$, *fr2/fr2*), the WPR-3 fertile revertant (*pvs*$^-$, *fr2/fr2*), and GO8063 (*pvs*$^+$, *Fr2/Fr2*) were analyzed simultaneously by ELISA. Fractionation of the anther protein involved size exclusion column centrifugation. Data presented in Table 1 indicate that a significant signal above basal level was observed in the anther protein preparation from CMS-Sprite only. Root mitochondrial protein preparations of CMS-Sprite gave an absorbance reading slightly above background. No other protein samples (total or mitochondrial protein preparations) demonstrated detectable cross-reactivity with the antibodies. Anther protein extracts from the fertile line GO8063, which contains the *orf239* sequence, did not indicate the presence of the Pvs-ORF239 protein. Protein preparations from the WPR-3 fertile revertant served as a negative control because the *pvs* sequence is absent from mitochondria in this line. Based on ELISA analysis, expression of Pvs-ORF239 was detectable only within anther tissues of the CMS-Sprite line, suggesting that Pvs-ORF239 is associated with sterility and is expressed in a tissue-specific manner.

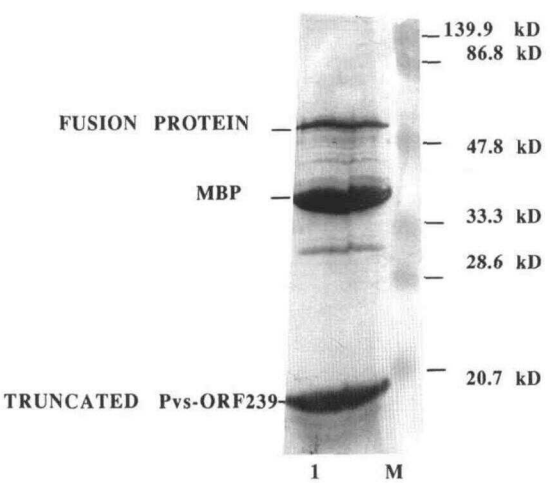

Figure 2. Characterization of Anti–Pvs-ORF239 Antibodies Using Gel Blot Analysis.

Lane M contains molecular mass standards. Lane 1 contains the cleaved fusion protein products that were subjected to SDS-PAGE followed by protein gel blotting. The immmunoblot was incubated with anti–Pvs-ORF239 antibodies. The antibodies cross-reacted with the uncleaved fusion protein (MBP with truncated Pvs-ORF239), MBP, and truncated Pvs-ORF239.

Table 1. ELISA Results Obtained with Protein Preparations Taken from Different Plant Tissues[a]

Tissue[b]	CMS-Sprite *pvs*$^+$, *fr2/fr2*	GO8063 *pvs*$^+$, *Fr2/Fr2*	WPR-3 *pvs*$^-$, *fr2/fr2*
Anther	0.685 ± 0.03[c]	0.151 ± 0.04	0.153 ± 0.05
Root	0.270 ± 0.02	0.170 ± 0.03	0.171 ± 0.02
Mature leaf	0.137 ± 0.04	0.143 ± 0.04	0.141 ± 0.04
Seedling	0.190 ± 0.02	0.170 ± 0.03	0.160 ± 0.03

[a] Absorbance is at 405 nm.

[b] Mitochondria were isolated from tissue of roots, mature leaves, and seedlings for analysis. Anther samples were size-fractionated protein preparations.

[c] Data represent the mean of two experiments with duplicate samples per experiment.

Size of Anther Protein Cross-Reacting with Anti–Pvs-ORF239 Antibodies

Mitochondrial protein preparations from root, etiolated seedling, and leaf tissues, along with fractionated protein samples from anthers, were used in the protein gel blot analyses. Root, seedling, and leaf protein samples were loaded at 1.5 times the amount of anther protein samples for gel electrophoresis. No cross-reactivity with anti–Pvs-ORF239 antibodies was detected in samples from the revertant WPR-3 or GO8063 line (data not shown). In CMS-Sprite samples, cross-reactivity was observed in the anther protein preparation only. Anti–Pvs-ORF239 antibodies did not recognize any proteins in root mitochondrial protein preparations of CMS-Sprite (data not shown). Figure 3 demonstrates that two protein bands, 27.5 and 21 kD in size, cross-reacted with the polyclonal antibodies in the protein preparations from dissected anthers of CMS-Sprite. Based on the DNA sequence, the expected molecular mass of the Pvs-ORF239 protein is 27 kD. The observed band at 27.5 kD should correspond to the intact ORF239 protein, whereas the lower molecular mass band may correspond to a degradation product or the result of protein cleavage during sample processing. The cross-reacting bands appeared diffused. This diffusion may be due to the nature of the hydrophobic N terminus of the protein (Konig and Sandermann, 1982). Anther protein preparations of neither revertant WPR-3 nor GO8063, loaded in 50% excess concentration compared with preparations from CMS-Sprite, demonstrated cross-reactivity with the anti–Pvs-ORF239 antibodies.

To evaluate the efficiency of intact mitochondrial protein extraction, a gel blot was probed first with anti–Pvs-ORF239 antibodies and then with anti-ATPA antibodies (ATPase α subunit). This gel blot analysis indicated that ATPA was present in all samples, whereas only CMS-Sprite had detectable levels of Pvs-ORF239 (data not shown). Consequently, protein gel blot experiments served to confirm the ELISA results, indicating that Pvs-ORF239 was present at detectable levels in anther tissues of CMS-Sprite only. These experiments also

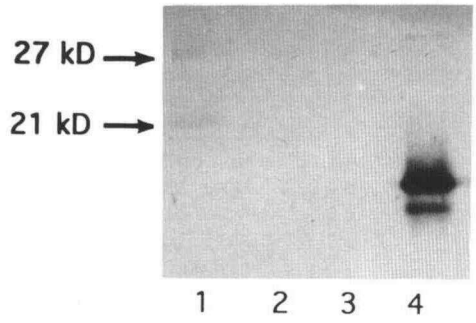

Figure 3. Characterization of the Proteins Cross-Reacting with Anti–Pvs-ORF239 Antibodies in Fractionated Anther Protein Preparations Using Gel Blot Analysis.

Proteins were separated by SDS-PAGE for gel blot analysis. Lane 1 contains the anther protein preparation from CMS-Sprite (80 μg). Lanes 2 and 3 contain WPR-3 and GO8063, respectively, loaded with 120 μg of sample protein. Lane 4 contains truncated Pvs-ORF239 protein. Arrows indicate the two CMS-Sprite proteins (27.5 and 21 kD) that cross-react with anti–Pvs-ORF239 antibodies. All lanes are from the same experiment.

demonstrated that the CMS-Sprite anther protein cross-reacting with anti–Pvs-ORF239 antibodies has a molecular mass equivalent to that of the predicted gene product of *pvs-orf239*.

Immunocytological Localization of Pvs-ORF239 in CMS-Sprite

To analyze further the expression pattern of Pvs-ORF239 during anther development, a detailed light microscopic examination of microsporogenesis was conducted. Floral buds of the three bean lines, CMS-Sprite, the WPR-3 revertant, and GO8063, were embedded in Quetol, sectioned to a thickness of 4 μm, and stained. At a premeiotic stage, all three lines appeared similar in anther development, as presented in Figures 4A and 4B (line GO8063, although not shown, yielded results identical to the revertant). At the onset of meiosis, however, the callose deposition layer in CMS-Sprite meiocytes appeared to be variable and, in many cases, substantially reduced relative to the callose layer in either the revertant or the GO8063 line. In common bean, callose is deposited around the pollen mother cell at early prophase I (Zhang and Xi, 1991). Sectioning of several CMS-Sprite floral buds revealed that callose deposition varied from a very thin layer (Figure 4C) to a much thicker one. The callose layer in the fertile line was consistently thicker and fully encased the products of meiosis (Figure 4D). These observations indicated that the effects of mitochondrial dysfunction might be evident already at premeiosis.

To verify that callose deposition was altered in CMS-Sprite, floral buds of CMS-Sprite, the revertant, and GO8063 were embedded in paraffin and stained with aniline blue for fluorescence microscopy. Fluorescence staining unequivocally demonstrated that callose deposition was significantly reduced and highly variable in the CMS-Sprite anthers. Examples of callose deposition in CMS-Sprite and the revertant WPR-3 are represented in Figures 4E and 4F. CMS-Sprite microspores, seen in Figure 4G, remained attached in the original tetrad configuration as described by Johns et al. (1992), in contrast to the release of free pollen in the revertant (Figure 4H) and GO8063 lines.

At the stage of callose deposition, immunocytochemistry by light microscopy was performed to determine whether Pvs-ORF239 was expressed. Sectioned bud tissues of CMS-Sprite, the WPR-3 revertant, and GO8063 were incubated at the microspore tetrad stage with anti–Pvs-ORF239 antibodies. As shown in Figure 5A, a strong signal was observed within the tetrads of CMS-Sprite, but no labeling was detected in the surrounding sporophytic tissues. The labeling appeared to be localized within the callose layer and in the developing cell walls of the microspores during cytokinesis. In contrast, tetrads of the revertant and GO8063 were unlabeled except for low-level background (Figure 5B; results from GO8063 were identical and not shown). When mature pollen was subjected to the same procedure, again, only CMS-Sprite pollen, retained as tetrads, was labeled as shown in Figure 5C. At no stage in development were floral bud tissues from the WPR-3 revertant or GO8063 found to be labeled (Figure 5D; GO8063 not shown). Based on these experiments, the anther-specific expression of Pvs-ORF239 was associated with the aborting tetrads in the CMS line.

Our analysis of CMS-Sprite anther tissues indicated that *pvs-orf239* is expressed only in CMS-Sprite and is associated with the pollen mother cells and developing microspores. However, CMS is a maternally transmitted phenotype. Consequently, we were interested in whether mitochondria transmitted to the next generation, contained within the ovules, also express Pvs-ORF239. Embedded buds from the three plant lines used in the previous study were sectioned longitudinally and immunologically evaluated. In CMS-Sprite bud sections, labeling of the ovules is presented in Figures 5E and 5F. No labeling was observed in GO8063 (data not shown) or in WPR-3 revertant (Figures 5G and 5H) ovule tissues. Labeling of the surrounding tissues was minimal and appeared to represent nonspecific background. These results suggest that expression of Pvs-ORF239 occurs in both developing female and male reproductive tissues of the CMS-Sprite bean line. Expression of Pvs-ORF239 in the ovules is intriguing because this organ has not yet been shown to display a sterility phenotype associated with *pvs*. Developmental differences between megasporogenesis and microsporogenesis, such as callose deposition, might render the male gametes susceptible to the effect of Pvs-ORF239.

To localize expression of Pvs-ORF239 more precisely, electron microscopic immunocytochemistry was performed using floral bud tissues from CMS-Sprite, the WPR-3 revertant, and GO8063 at the premeiotic tetrad and mature pollen stages. At

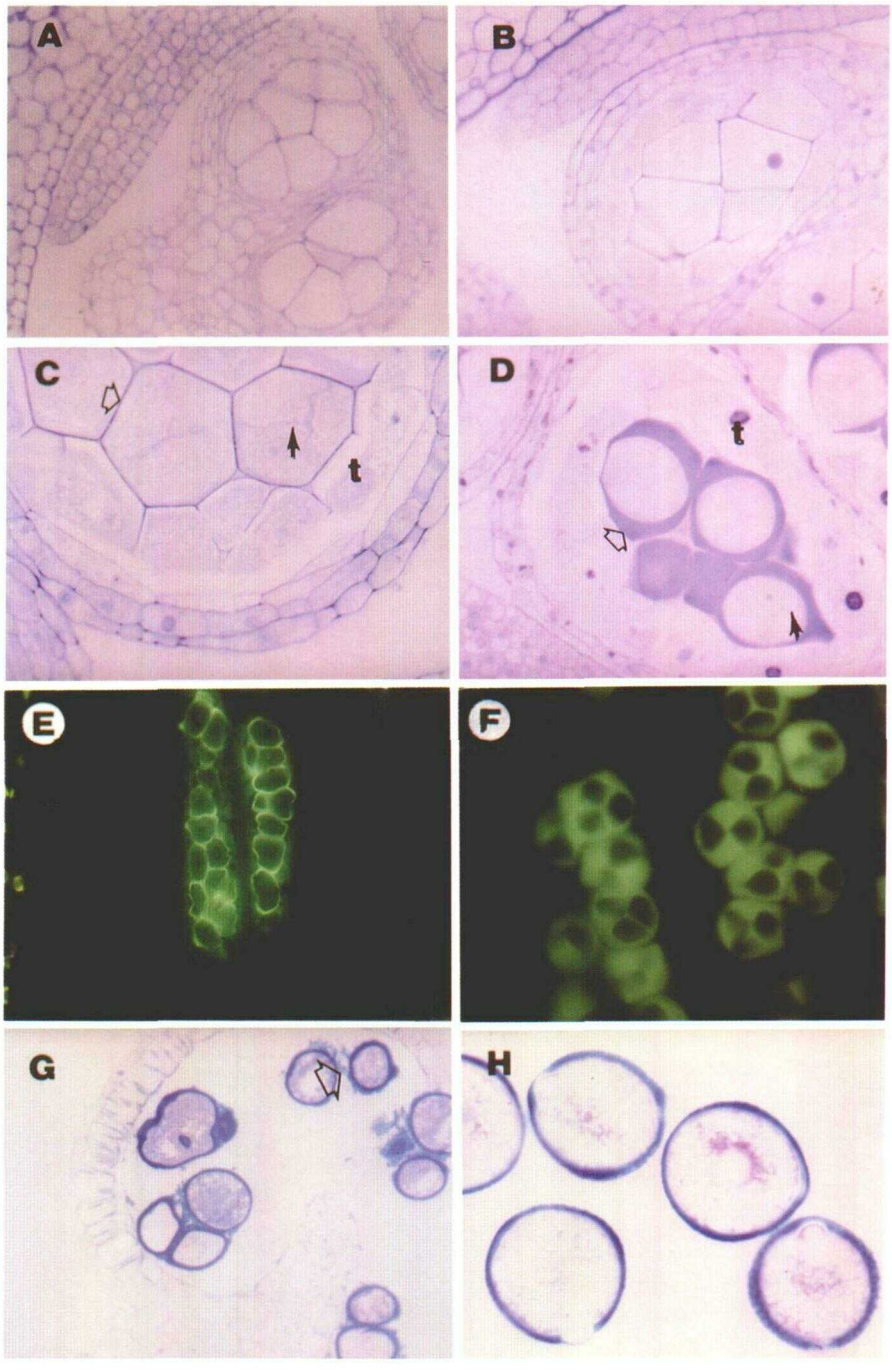

Figure 4. Histological Evaluation of Developing Microspores of CMS-Sprite and WPR-3.

Flower buds collected at various stages of microspore development were embedded in either Quetol or paraffin, sectioned, and stained with toluidine blue O. **(A)**, **(C)**, **(E)**, and **(G)** represent samples of CMS-Sprite as compared with the fertile revertant (*pvs*$^{-}$) in **(B)**, **(D)**, **(F)**, and **(H)**. Results from the fertile restored line GO8063 (similar to those from WPR-3) are not shown.

(A) and **(B)** Developing pollen mother cells. Magnifications are ×148 and ×220, respectively.

(C) and **(D)** Aberrant callose deposition observed in CMS-Sprite compared with normal callose deposition in the revertant at late meiosis. The primary cell walls separating the microspores are evident in both micrographs. Open arrows indicate the site of the callose layer, and solid arrows indicate the developing primary cell walls; t represents the tapetal layer. Magnifications are ×370 and ×300, respectively.

(E) and **(F)** Callose at the same stage shown in **(C)** and **(D)** stained with aniline blue for fluorescence microscopy. Aberrant deposition in CMS-Sprite is evident. Magnifications are ×70 and ×150, respectively.

(G) and **(H)** Developing microspores. Microspores are retained as tetrads in CMS-Sprite throughout development. The open arrow indicates the remaining cell wall between them. In WPR-3, microspores are separated. Magnifications are ×360 and ×740, respectively.

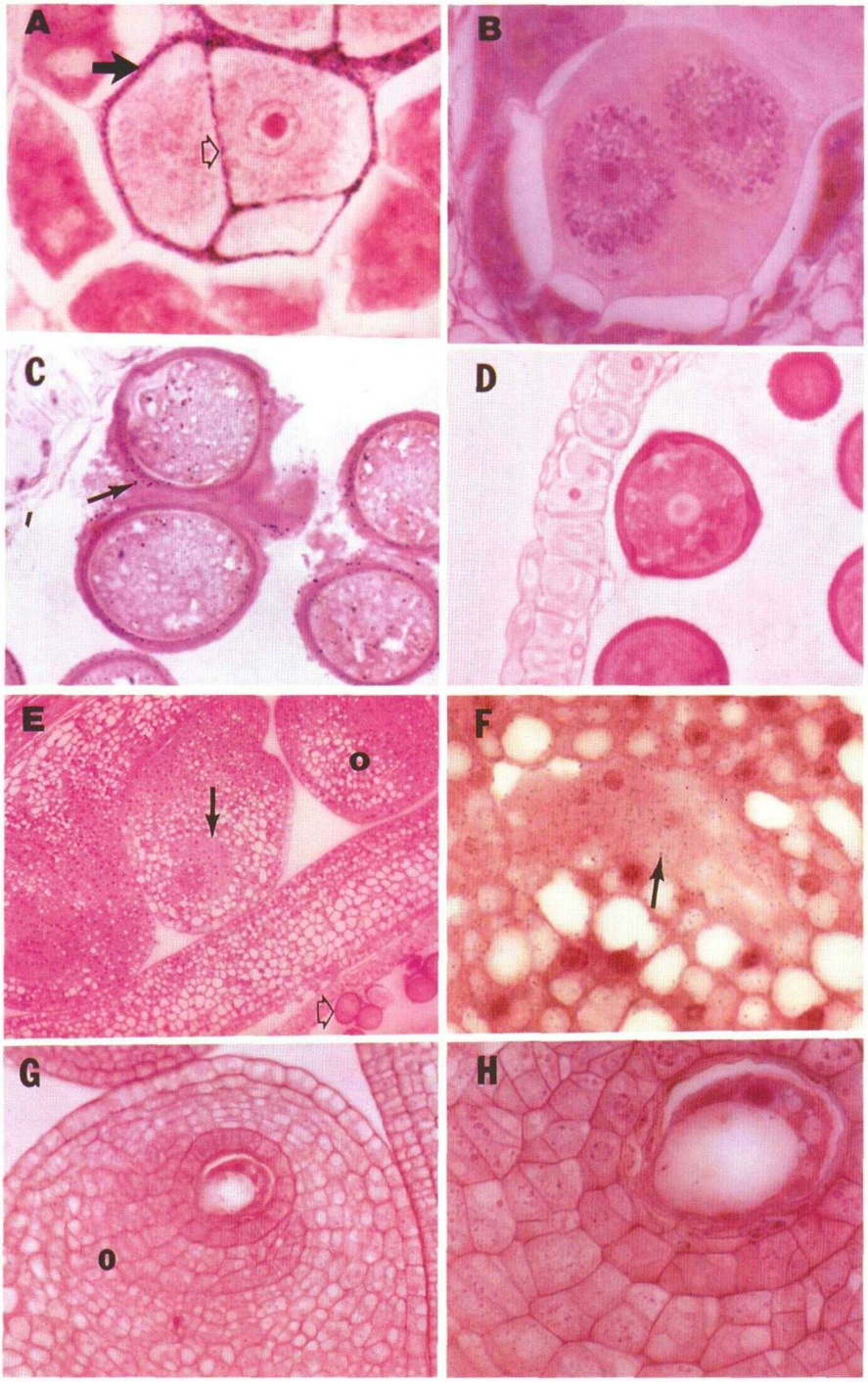

Figure 5. Light Microscopic Immunocytochemistry of Developing Microspores and Ovules in CMS-Sprite and WPR-3.

Developing bud tissues from CMS-Sprite shown in **(A)**, **(C)**, **(E)**, and **(F)** and the WPR-3 revertant in **(B)**, **(D)**, **(G)**, and **(H)** were embedded in Quetol, sectioned, and incubated with anti–Pvs-ORF239 antibodies. Primary antibody detection involved incubation with gold-conjugated goat anti–rabbit IgG, followed by silver enhancement. Results from GO8063 were similar to those from WPR-3 and are not shown.

(A) and **(B)** *Antibody preferentially labels the CMS-Sprite callose layer (solid arrow) and primary cell wall (open arrow).* No gold particles were detected in the WPR-3 revertant. Magnification is ×940 for **(A)** and **(B)**.

(C) and **(D)** Antibody labeling is still present in the cell wall of the developing microspores (solid arrow in **[C]**) and the cytoplasm of CMS-Sprite. Cross-reactivity was not observed in WPR-3 revertant microspores **[(D)]**. Magnification is ×780 for **(C)** and **(D)**.

(E) and **(F)** CMS-Sprite ovules are shown. The open arrow in **(E)** *indicates the microspores in tetrads that serve as a positive* labeling control. The solid arrow in **(E)** indicates the site of enlargement demonstrated in **(F)**. The solid arrow in **(F)** indicates the location of the gold particle in the ovule. O represents the ovule. Magnifications are ×160 and ×935, respectively.

(G) and **(H)** The WPR-3 ovule shows no labeling in contrast to the ovule of CMS-Sprite. GO8063 ovules also demonstrated no cross-reactivity (data not shown). O represents the ovule. Magnifications are ×312 and ×780, respectively.

premeiotic stages, pollen mother cells of CMS-Sprite contained well-defined mitochondria sparsely labeled by anti–Pvs-ORF239 antibodies, as presented in Figure 6A. Evaluation of 15 micrographs taken at random indicated that, per square millimeter, 85% of the labeling detected was within mitochondria. Mitochondria from the WPR-3 revertant (Figure 6B) and GO8063 (data not shown) displayed no cross-reactivity with the antibodies except for low-level nonspecific background. Approaching meiosis, as the mitochondria began to lose their well-defined cristae, labeling in the meiocytes increased drastically in CMS-Sprite. Figures 6C and 6D show that gold particles were localized both in the cytoplasm and within mitochondria. Mitochondria of CMS-Sprite at this stage contained intricate, dense, and amorphous deposits as indicated in Figure 6D. Antibody labeling was observed in neither the revertant nor the GO8063 cells at this stage (data not shown).

At the onset of callose deposition, intense cross-reactivity of the anti–Pvs-ORF239 antibodies with the callose layer was observed in the male-sterile bean line, together with labeling of the developing primary cell wall (Figure 6E). Gold particles continued to be evident in the cytoplasm and the mitochondria of CMS-Sprite. After meiosis, callose surrounding the developing microspores in the WPR-3 revertant and GO8063 was removed, and the individual pollen grains were released into the anther locule. In contrast, CMS-Sprite pollen remained in tetrads, apparently bound together by primary cell wall material (Figure 6F). Cytokinesis was often incomplete, and the mitochondria remained dedifferentiated (cristae not visible). Intense labeling of the undissolved callose layers, the primary cell walls, and degenerated mitochondria persisted until abortion in CMS-Sprite. This phenomenon was not observed in GO8063 (Figure 6G) or in WPR-3 (data not shown). Incubation of the samples with anti-MBP (data not shown) and anti-ATPA antibodies (Figure 6H) or with preimmune serum produced no labeling of the callose layer or developing meiocyte cell walls. Together, results from these experiments indicated that expression of Pvs-ORF239 within developing pollen of CMS-Sprite is associated with mitochondria and, surprisingly, also with the developing callose layer and microspore wall.

Interaction of Pvs-ORF239 with Cell Wall Preparations

The localization of Pvs-ORF239 in the callose layer and the cell wall during microspore cytokinesis was shown by both light and electron microscopy immunocytological analyses. To investigate further the specificity of the interaction of Pvs-ORF239 with the cell wall of CMS-Sprite, cell wall preparations of CMS-Sprite, the WPR-3 revertant, and tobacco were obtained from suspension cultures. The cell wall preparations were incubated in the presence or absence of the purified Pvs-ORF239 expression product (Pvs-ORF239 truncated form). Protein gel blot analysis of the supernatant solution after incubation of cell walls with Pvs-ORF239 indicated that Pvs-ORF239 was depleted from the solution in all three cell wall preparations (data not shown). Incubation of the cell walls with the protein mixture consisting of MBP, the fusion protein, and Pvs-ORF239 (truncated) was also conducted. Gel blot analysis revealed that only MBP remained in solution, whereas Pvs-ORF239 and the fusion protein were removed from the solution upon pelleting of the cell walls (Figure 7).

Cell wall preparations were incubated with purified, truncated Pvs-ORF239, subsequently washed several times with buffer, and treated with anti–Pvs-ORF239 antibodies. Immunocytochemistry was performed with the three cell wall preparations. Omission of the Pvs-ORF239 protein incubation in all three cell wall samples resulted in a lack of antibody labeling as shown in Figure 8A, whereas incubation of the cell wall preparations with Pvs-ORF239 resulted in extensive gold particle deposition, as indicated by Figures 8B and 8C. Controls omitting anti–Pvs-ORF239 antibodies (data not shown), secondary goat anti–rabbit IgG (Figure 8D), or both primary and secondary antibodies (data not shown) also produced no signal. It should be pointed out that boiling the cell wall preparation in SDS after incubation with Pvs-ORF239 resulted in no detectable release of Pvs-ORF239 protein (data not shown). These data show that Pvs-ORF239 precipitates with, and apparently binds to, cell wall preparations of not only CMS-Sprite, but also the WPR-3 revertant and tobacco. The same experiments were duplicated using MBP and anti-MBP antibodies (New England Biolabs, Beverly, MA). No labeling of the cell wall preparations was detected (data not shown), indicating that our conditions did not favor nonspecific binding of proteins to the cell wall preparation.

DISCUSSION

Tissue-specific changes in the expression of mitochondrial genes (Conley and Hanson, 1994; Smart et al., 1994) and of nuclear genes encoding mitochondrial products (Johns et al., 1993; Huang et al., 1994) have been recently demonstrated in higher plants. Tissue-specific expression of a CMS-associated peptide has not been previously reported. This study presents three important observations. First, we have demonstrated tissue-specific expression of a mitochondrial peptide associated with pollen sterility. Second, the results indicate that a fertile plant line containing the mitochondrial sterility-associated sequence *pvs* does not appear to express Pvs-ORF239 in the presence of the nuclear restorer gene *Fr2*. Finally, these results demonstrate that Pvs-ORF239 is found both in developing pollen of the male-sterile line and in female reproductive tissues.

It has been suggested that expression of the *pvs* sequence causes pollen sterility in common bean (Mackenzie and Chase, 1990; Mackenzie, 1991; Johns et al., 1992). The current study localized the Pvs-ORF239 protein within the reproductive tissues of the male-sterile plant CMS-Sprite. Furthermore, the Pvs-ORF239 peptide was found to be associated with mitochondria during microsporogenesis. These observations imply that the Pvs-ORF239 protein plays a role in the sterility phenotype observed in CMS-Sprite. However, the *orf239* sequence

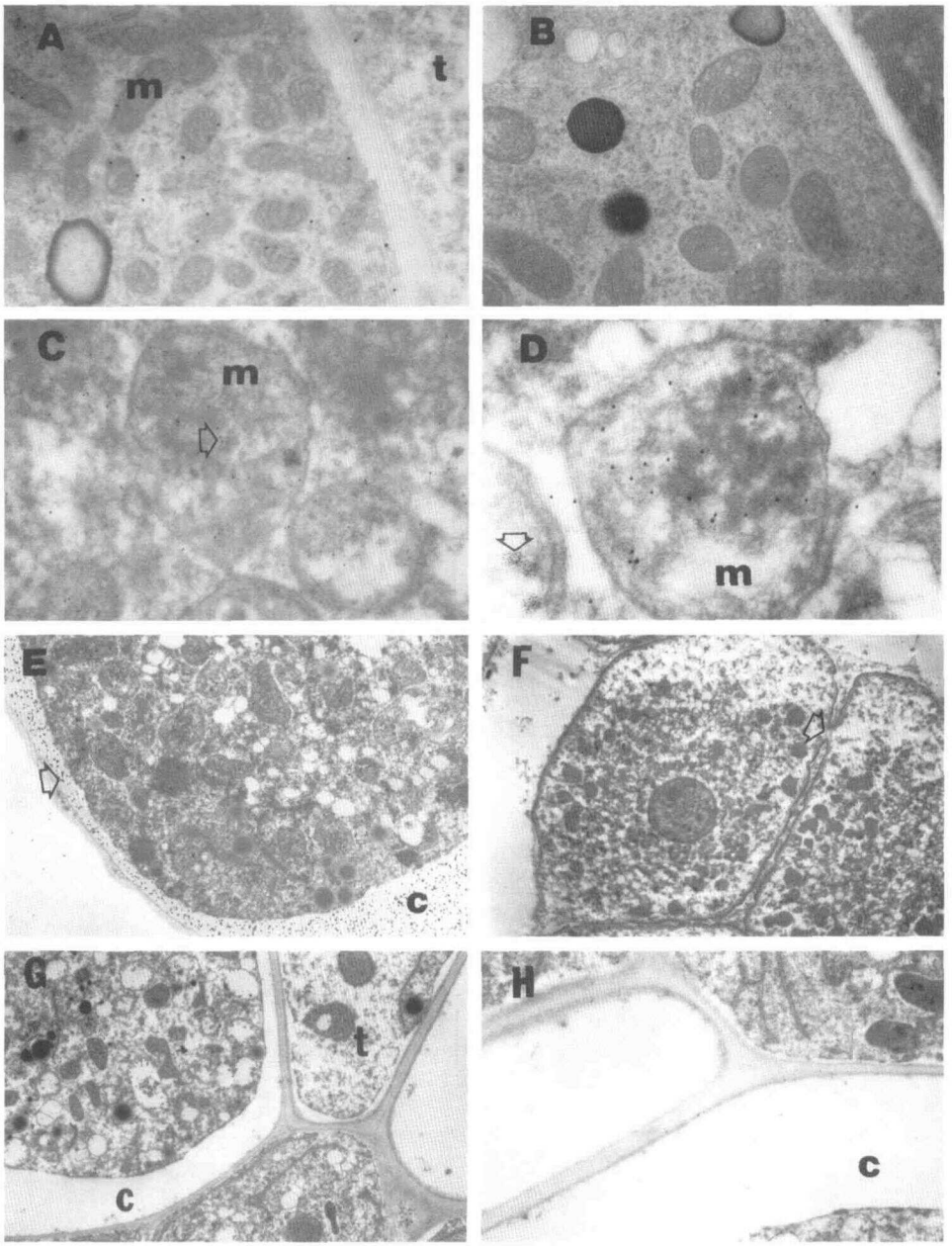

Figure 6. Immunogold Localization of Pvs-ORF239 in CMS-Sprite.

Buds were embedded in Quetol, sectioned, and then incubated with anti–Pvs-ORF239 antibodies. Primary antibody detection involved incubation with gold-conjugated goat anti–rabbit IgG.

(A) Premeiotic buds from CMS-Sprite with sparse labeling of mitochondria. Magnification is ×12,600.

(B) WPR-3 control at the same stage with no cross-reactivity. Magnification is ×14,300.

(C) and **(D)** Antibody labeling within the mitochondria of CMS-Sprite. In **(C)**, the open arrow indicates gold particles. In **(D)**, the open arrow indicates amorphous deposits within the mitochondria. Magnifications are ×30,200 and ×35,300, respectively.

(E) Immunogold antibody labeling of the developing callose (c) layer in CMS-Sprite. The open arrow indicates the area of cross-reactivity. Magnification is ×5900.

(F) Postmeiosis stage in CMS-Sprite leading to incomplete cytokinesis. The open arrow shows the lack of normal cell wall deposition. Magnification is ×2100.

(G) Callose layer in GO8063 incubated with anti–Pvs-ORF239 antibodies. No cross-reactivity is evident. Magnification is ×4200.

(H) Control of CMS-Sprite incubated with anti-ATPA antibodies. No labeling within the callose layer is evident. Magnification is ×6700.

m, mitochondria; t, tapetum; c, developing callose layer.

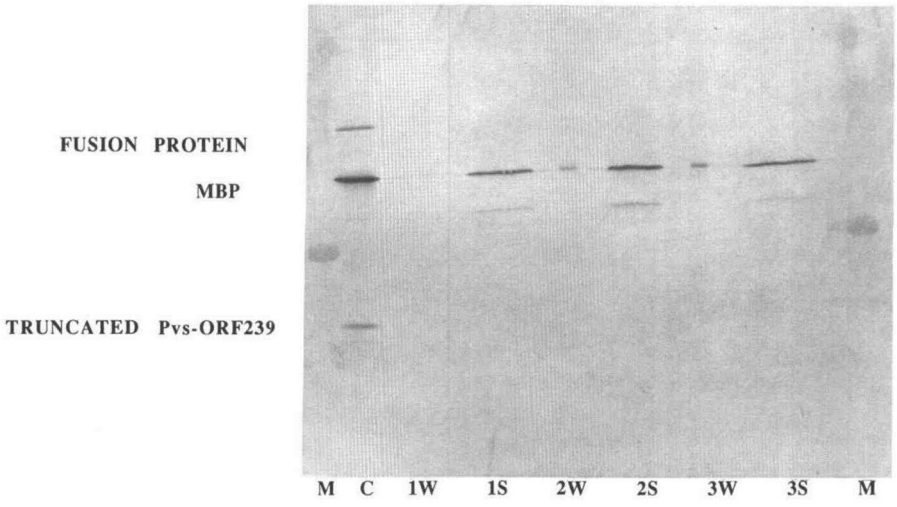

Figure 7. Depletion of Pvs-ORF239 from Protein Solution by Cell Wall Preparations.

Protein solutions containing uncleaved fusion protein, MBP, and truncated Pvs-ORF239 were mixed with cell wall preparations from CMS-Sprite, the WPR-3 revertant, and tobacco (cv W38). Gel blot analysis was performed. Lanes M correspond to the molecular mass markers. Lane C (control) is the control starting protein sample with uncleaved fusion protein, MBP, and truncated Pvs-ORF239. CMS-Sprite is sample 1, tobacco is sample 2, and WPR-3 is sample 3. Lanes 1W, 2W, and 3W (washes) were obtained after washing the cell wall samples with buffer after incubation with the solution from lane C. Lanes 1S, 2S, and 3S (supernatant) were the supernatants of the solution after incubation of the starting protein preparation with the cell wall samples.

represents only one of two ORFs cotranscribed from the unique *pvs* region (Chase and Ortega, 1992; Johns et al., 1992). The predicted product of the second *pvs*-encoded ORF, Pvs-ORF98, has not been characterized, and its role, if any, in sterility is not known. The possibility that a combined effect of Pvs-ORF98 and Pvs-ORF239 causes the pollen sterility phenotype cannot be ruled out. Investigation into the expression of *pvs-orf98* is needed to determine whether this sequence is also important to male sterility.

The association of Pvs-ORF239 with the callose layer and the primary cell wall of CMS-Sprite developing microspores was unexpected. Because our experiment to localize Pvs-ORF239 included isonuclear lines CMS-Sprite and the revertant WPR-3, the possibility that the cross-reaction observed is due to a cellular wall–bound protein of nuclear origin is highly unlikely. Subsequent experiments to test the specificity of this Pvs-ORF239 affinity for the cell wall indicated that the truncated form of Pvs-ORF239 had a strong affinity for cell walls of not only CMS-Sprite, but also the WPR-3 revertant and even tobacco. It can be concluded from these experiments that the association of Pvs-ORF239 with the cell wall, at least in vitro, does not result from unique biochemical properties of the CMS-Sprite pollen wall. Rather, these results imply a general affinity of the protein for wall or callose materials. How the Pvs-ORF239 protein, presumably secreted or released from the mitochondria by lysis, is able to move to the periphery of the cell is not clear.

It cannot yet be concluded that the abnormal pattern of pollen development is a direct consequence of the association of Pvs-ORF239 with the developing pollen wall. This unusual association of Pvs-ORF239 with the callose layer and the primary wall may be a secondary effect of *orf239* expression. The presence of a hydrophobic stretch of amino acids at the N terminus of Pvs-ORF239 suggests an association with the inner mitochondrial membrane to cause mitochondrial dysfunction. Nevertheless, one cannot ignore the data from light and electron microscopy studies indicating that the earliest phenotypic distinctions between CMS-Sprite and the isonuclear WPR-3 fertile revertant occur at the point of callose deposition prior to meiosis. Whether the accumulation of Pvs-ORF239 within the callose layer influences the pattern of callose deposition in CMS-Sprite is not yet known. We are investigating this question using plant transformation experiments in which gene constructs containing the Pvs-ORF239 sequence with and without a mitochondrial transit sequence will be introduced to plants. These subsequent experiments should indicate not only whether expression of Pvs-ORF239 is sufficient to result in abnormal pollen development, but also whether the localization of Pvs-ORF239 within the callose layer and pollen wall, bypassing the mitochondrion altogether, can cause the observed developmental change.

The localization of Pvs-ORF239 to the callose layer was unexpected for a second reason. In an earlier study, Johns et al. (1992) reported that abnormal pollen development in CMS-Sprite appeared to be associated with incomplete cytokinesis. The primary cell wall between microspores appeared to be perforated and allowed cytoplasmic connections to be retained between microspores. It was also demonstrated that

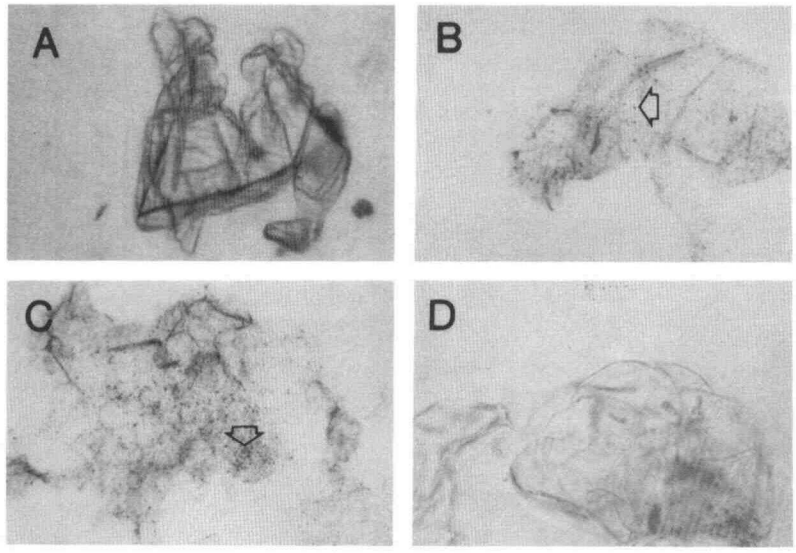

Figure 8. Affinity of Pvs-ORF239 for Purified Cell Walls.

(A) Purified cell walls (CMS-Sprite) not incubated with Pvs-ORF239, but exposed to anti–Pvs-ORF239 antibodies, incubated with gold-conjugated goat anti–rabbit IgG, and silver enhanced.
(B) Cell wall preparation (CMS-Sprite) incubated with Pvs-ORF239 and centrifuged, given multiple washes, and treated as described in **(A)**.
(C) Immunolocalization of Pvs-ORF239 within cell wall samples of tobacco (cv W38) that were processed as given in **(B)**.
(D) Cell wall preparations from CMS-Sprite treated with Pvs-ORF239. Secondary antibodies were omitted.
Open arrows indicate gold particle labeling as a positive reaction. Magnification is ×320 in **(A)** to **(D)**.

pollen abortion as tetrads did not occur until much later in development after pollen mitosis. No differences in callose deposition between CMS-Sprite and normal fertile lines were reported. However, this previous study emphasized postmeiotic development. It was only after detailed observation of the pollen mother cells at the onset of meiosis in this study that the abnormally thin callose layers in CMS-Sprite were noticed. The modifications in pollen development patterns that occur before meiosis while pollen continues to develop to the binucleate stage suggest that the changes in callose and primary wall deposition are the first observable consequence of mitochondrial dysfunction in male-sterile CMS-Sprite. Pollen abortion as well as visible evidence of mitochondrial degeneration (data not shown) occur much later in the process.

To date, relatively little is understood about the mechanism controlling callose and pollen wall deposition. Studies of pollen development under conditions of premature callose dissolution, using transgenic plants containing a gene construct for β-1,3-glucanase, have demonstrated a close association between callose and the development of the primary pollen wall (Worrall et al., 1992). Microspores in which callose dissolved early were unable to produce normal primexine and aborted. It is not clear, however, whether abnormal callose deposition, while resulting in tetrad pollen, necessarily leads to pollen abortion. In some plant species (Blackmore and Crane, 1988) and derived mutants (Preuss et al., 1994), unusual patterns of callose deposition can lead to viable pollen shed in tetrads. Data are now accumulating to indicate the important roles played by a number of previously unknown proteins in cell wall modification (for example, see Fry et al., 1992; McQueen-Mason et al., 1992). The possibility exists that Pvs-ORF239 could interfere with or mimic a protein required for callose deposition.

Previous studies have demonstrated that fertile accession line GO8063 contains a sterility-inducing cytoplasm apparently identical to that of CMS-Sprite (Mackenzie, 1991). GO8063 was shown to be fertile by virtue of the presence of a nuclear fertility restorer gene, *Fr2*. Yet, transcriptional analysis indicates that the *pvs* transcript pattern is identical in CMS-Sprite and GO8063 seedlings (Mackenzie and Chase, 1990) and floral buds (Chase, 1994). Results of this study, indicating nondetectable levels of Pvs-ORF239 in GO8063, imply that *Fr2* influences expression of Pvs-ORF239 translationally or post-translationally. It is important to note, however, that CMS-Sprite and GO8063 are not isonuclear lines. Consequently, it will be necessary to compare CMS-Sprite and CMS-Sprite-*Fr2* near-isolines to define better the role of *Fr2*.

It should be pointed out that translational or post-translational control of *pvs* expression most likely occurs even in the absence of restorer gene *Fr2*. Earlier studies (Mackenzie and Chase, 1990; Chase, 1994) have demonstrated that *pvs* transcripts are present in young seedling and floral tissues of the CMS-Sprite plant. Furthermore, these transcripts apparently associate with polysomes in both tissues (Chase, 1994). Yet, this study demonstrates that the Pvs-ORF239 protein is not present in the young seedling, which implies that translational

regulation or rapid protein turnover could account for the lack of Pvs-ORF239 in tissues other than reproductive ones.

A second fertility restoration system has been genetically characterized for CMS in common bean. Restoration of normal pollen development by *Fr* is accompanied by the loss of a large portion of the mitochondrial genome encompassing *pvs* (Mackenzie and Chase, 1990; Janska and Mackenzie, 1993). Developmental analysis of this restoration process shows that complete loss of *pvs* occurs during pollen and ovule development (He et al., 1995). More significant to the results of this study, He et al. (1995) proposed a model suggesting that *Fr* action is dependent on the expression of the *pvs* sequence. This model is derived from the observation that in the presence of the restorer gene *Fr2*, introduction of *Fr* no longer effects the loss of *pvs*. This model makes two important predictions. First, *Fr2* must reduce or eliminate expression of the *pvs* sequence; second, the *pvs* sequence must be expressed not only in the developing microspores, causing pollen abortion, but also during megasporogenesis. This is because the restorer gene *Fr* has two effects: to restore pollen viability and to prevent transmission of the *pvs* sequence to the subsequent generation. We have demonstrated that the Pvs-ORF239 protein is, in fact, not present in *Fr2/Fr2* (GO8063) plants. Also consistent with this model, Pvs-ORF239 expression was detected not only in pollen but also in the ovules of CMS-Sprite buds.

One final observation from this study is significant to the modeling of nuclear restorer gene action. Genetic analysis indicates that the fertility restorer gene *Fr* behaves as a sporophytic restorer (acts in 2N tissue) (Mackenzie and Bassett, 1987), as does *Fr2* (Mackenzie, 1991). Hence, it is important to point out that Pvs-ORF239 expression was detected during premeiosis in the developing meiocytes. The significance of this observation is its implication that fertility restoration processes effected by *Fr* and *Fr2* are likely to occur during the brief period of Pvs-ORF239 expression just prior to meiosis.

Based on the results from this study, we can conclude that Pvs-ORF239 is associated with male sterility in common bean. Expression of this mitochondrial protein was observed only in the reproductive tissues of CMS-Sprite, indicating that its expression is tissue specific. The lack of Pvs-ORF239 in the fertile GO8063 line containing the *pvs* sequence supports our earlier assumption that Pvs-ORF239 is post-transcriptionally regulated by *Fr2*. Observations from this study now provide the basis for direct investigation of the cellular processes leading to pollen abortion and suggest that the molecular basis of fertility restoration will be experimentally approachable in this system.

METHODS

Plant Materials

Three lines of common bean (*Phaseolus vulgaris*) were used. The fertile line GO8063 contains the sterility-inducing cytoplasm (*pvs*$^+$) and the nuclear restorer gene *Fr2* (Mackenzie, 1991). The CMS-Sprite line was derived from a cross of GO8063 × cultivar Sprite followed by backcrossing, with Sprite (maintainer line) as the pollinator for 16 generations (Singh et al., 1980; Bassett and Shuh, 1982). WPR-3 is a spontaneous fertile revertant of the cytoplasmic male-sterile line (CMS) that has lost a large portion of the mitochondrial genome encompassing the *pvs* sequence (Janska and Mackenzie, 1993). CMS-Sprite and WPR-3 are isonuclear lines.

Protein Preparations

Young etiolated seedlings were grown on vermiculite for 7 days in complete darkness. Seedling roots, etiolated hypocotyls, greenhouse-grown mature leaves, and dissected anthers of the three plant lines were used for protein preparations. The tissues were frozen in liquid nitrogen and ground to a fine powder. The ground samples were suspended in 10 mM Tris-HCl buffer, pH 6.8, 0.1% Tween 20. After centrifugation at 5000*g* for 30 min at 4°C, the supernatant was recovered and stored at −20°C. Mitochondria were purified from roots, leaves, and young seedlings as previously described (Mackenzie and Chase, 1990). The mitochondrial samples were processed by the same protocol described previously and stored at −20°C. Protein from dissected anther preparations was concentrated by Centricon filtration (Amicon, Inc., Beverly, MA). The samples were first centrifuged using Centricon-100 at 1000*g*, which eliminated proteins with molecular mass greater than 85 kD. The filtrate was collected and centrifuged through Centricon-10 at 4500*g* to concentrate the anther proteins. These centrifugation steps size fractionated the dissected anther preparations from 85 to 10 kD. Protein concentration was determined using the Bradford protein assay (Bradford, 1976; reagent supply from Bio-Rad).

Cloning of the *pvs* Sequence

The *orf239* sequence, when cloned in its entirety and transformed to an *Escherichia coli* host, was highly unstable. Consequently, a truncated form of *pvs-orf239* was used. Primers for the polymerase chain reaction (PCR) amplification were developed as follows: primer 5′-GTTTGGAACTGGAATTCAGCTTGCACATGC-3′ anneals to the template at nucleotides 2408 to 2437 (Johns et al., 1992) to introduce an EcoRI site; primer 5′-TAGTAAAGGTTGCCCCATTAGCGGGGATGC-3′ anneals to the template at nucleotides 2876 to 2905 to introduce a HindIII site. The PCR product encodes Pvs-ORF239 minus the first 82 amino acids. The PCR product was digested with EcoRI and HindIII (Promega) according to manufacturer's instructions, ligated to the pMALc vector (New England Biolabs, Beverly, MA), and transformed to host cell line TB-1. Transformants were selected on Luria-Bertani (X-gal/ampicillin/isopropyl β-D-thiogalactopyranoside) medium with replica plating to Luria-Bertani (ampicillin) plates minus inducer. The cloned *orf239* sequence was determined to be in-frame to the upstream maltose binding protein (*MBP*) gene by DNA sequence analysis (Sequenase; U.S. Biochemical Corp.).

Pvs-ORF239 Purification

Transformed bacteria containing the truncated Pvs-ORF239 sequence in-frame with and 3′ to the *MBP* gene were grown according to the supplier's instructions (New England Biolabs). In brief, the bacterial culture was grown in a medium containing 10 g of tryptone, 5 g of yeast extract, 5 g of NaCl, and 2 g of glucose per liter, with an ampicillin concentration of 100 μg/mL. Bacteria were incubated at 36°C to a cell

optical density of 0.5 at 600 nm, and isopropyl β-D-thiogalactopyranoside was added to a final concentration of 0.3 mM. After 3 hr, the culture was harvested by centrifugation at 4000*g* for 20 min and resuspended in lysis buffer consisting of 10 mM phosphate, 30 mM NaCl, 0.25% Tween 20, 10 mM β-mercaptoethanol, pH 7.0. The cells were frozen at −20°C overnight. The thawed bacterial suspension was sonicated, NaCl was added to a final concentration of 0.5 M, and the suspension was centrifuged at 9000*g* for 30 min. The supernatant, at a protein concentration of 2.5 mg/mL, was loaded onto an amylose resin column. Protein was eluted with maltose-containing buffer and collected in 2.5-mL fractions. The fractions containing the fusion protein were identified using the Bradford protein assay (Bradford 1976; reagent supplied by Bio-Rad).

After denaturation of the fusion protein, cleavage MBP from Pvs-ORF239 was accomplished using factor Xa according to the protocol of the supplier (New England Biolabs). The cleavage product was assayed by SDS-PAGE on a 12% polyacrylamide gel. Coomassie blue staining of the first two lanes allowed verification of the Pvs-ORF239 protein at 17.5 kD. The remaining sample was cut from the gel and loaded into a GE200 Sixpac gel eluter (Hoefer Scientific Instruments, San Francisco, CA) for protein elution according to manufacturer's instructions. The purified Pvs-ORF239 truncated protein was used for rabbit immunization and experimental standard.

Antibody Production and Characterization

After bleeding for preimmune serum, the rabbit was injected with 150 μg/300 μL of fusion protein in complete Freund's adjuvant; 3 weeks later, the rabbit was injected with the purified Pvs-ORF239 truncated protein (50 μg/300 μL) in incomplete Freund's adjuvant. After three inoculation boosters, the antiserum was used to determine the titer and the specificity of the antibodies against the Pvs-ORF239 protein with the indirect procedure of ELISA.

ELISA Analysis

A 200-ng sample of protein (200 ng/100 μL) in coating buffer (1.59 g of Na_2CO_3, 2.93 g of $NaHCO_3$ per liter, pH 9.6) was loaded to each well in an ELISA microtiter plate (Corning Glass Works, Corning, NY). After a 2-hr incubation at 37°C, the plates were washed three times by flooding with PBS–1% Tween 20. The anti–Pvs-ORF239 antibodies in PBS–Tween 20 were added and incubated for 2 hr at 37°C. After several washes with buffer, alkaline phosphatase–labeled anti–rabbit goat IgG (Vector Laboratories, Burlingame, CA) was introduced into the well for 1 hr. Cross-reactivity was detected with the addition of a freshly prepared solution of p-nitrophenyl phosphate (Sigma) after thorough washing. The volume in all steps was kept at 100 μL. The plates were read at A_{405nm}. To standardize protein concentration in wells containing purified truncated Pvs-ORF239, BSA was added to raise the protein concentration to 200 ng/100 μL (1 to 10 ng of purified Pvs-ORF239 was added per well).

Protein Gel Electrophoresis and Blot Analyses

Heat-denatured protein samples in 6 × loading buffer (375 mM Tris buffer, pH 6.8, 12% SDS, 30% β-mercaptoethanol, 25% glycerol) were loaded into 12% acrylamide vertical slab gels (Protean II; Bio-Rad) for SDS-PAGE analysis (Laemmli, 1970). Electrophoresis was performed at constant current of 15 mA for 7 hr, with cooling at 4°C. The acrylamide gel was blotted to polyvinylidene difluoride membrane (Bio-Rad) using the wet procedure (Towbin et al., 1979) with Towbin buffer (25 mM Tris, pH 8.3, 192 mM glycine, 20% ethanol). The rapid transfer was performed at 100 mA for 1 hr. The membrane was incubated in Tris-HCl, pH 7.5, 0.8% NaCl, and 10% dried milk at 4°C overnight. After several washes, the membrane was incubated at 37°C with the anti–Pvs-ORF239 antibodies in a hybridization oven (Hybaid; National Labnet Company, Woodbridge, NJ) for 2 hr. The antibodies were diluted in Tris-HCl (optimal dilution empirically determined), pH 7.5, 1% NaCl, and 1% dried milk. After three washes for 5 min each, biotinylated goat anti–rabbit antibodies were added for 45 min, followed by several buffer washes and then by incubation with a solution of reagent containing avidin DH and biotinylated enzyme according to the supplier's instructions (ABC elite peroxidase kit 6101; Vector Laboratories). Color detection was achieved using horseradish peroxidase substrate solution containing 0.02% hydrogen peroxide and 0.1% diaminobenzidine tetrahydrochloride in 0.1 M Tris buffer, pH 7.2 (kit SK-4100; Vector Laboratories).

After hydration with PBS buffer, a gel blot previously incubated with anti–Pvs-ORF239 was probed with anti-ATPA antibodies (α subunit of ATPase). The blot was then treated with biotinylated goat anti-rabbit antibodies solution and, after several washes with buffer, incubated with avidin DH and biotinylated alkaline phosphatase H solutions (alkaline phosphatase kit AK-5001; Vector Laboratories). Color detection was achieved by hydrolysis of phosphate-containing substrate by alkaline phosphatase (kit II SK-5200; Vector Laboratories) according to the supplier's recommendation.

Light and Electron Microscopy Immunocytochemistry

Floral buds collected from CMS-Sprite, the WPR-3 revertant, and GO8063 were processed and embedded in Quetol (Ladd Research Industries, Burlington, VT) as previously described (Abad et al., 1988). Sections, 4 to 6 μm thick, were obtained, transferred to a droplet of water sitting on a slide, and then adhered to the slide with heat (75°C). For cytological analysis, the sections were stained with 1% toluidine blue O in 50% aqueous ethanol with 1% sodium borate, washed, dried, and mounted with Permount (Fisher Scientific). Thick sections of the floral buds, used for immunocytochemistry, were washed in PBS buffer, pH 7.4, 0.8% NaCl, 0.1% Tween 20 for 30 min, incubated with the anti–Pvs-ORF239 antibodies for 1 hr, rinsed, and incubated with goat anti–rabbit IgG labeled with gold particles of 15 and 30 nm. Amplification of the gold labeling was achieved with the Intense M silver enhancement kit (Amersham Life Science, Inc., Arlington Heights, IL). The enhancement process was monitored visually with the light microscope, and the reaction was allowed to proceed for only 2 min at a time. The process was repeated three times for each slide. This stepwise enhancement was found to produce adequate signal without significant background or undesirable silver nucleation and silver deposition onto the slides. The sections were then stained with aqueous 1% safranin O, 30% ethanol, to enhance contrast between the sample and the silver staining.

For electron microscopy immunocytochemistry, thin sections of the floral buds were mounted onto nickel grids and treated (Abad, 1992). Briefly, after floating the grids on PBS buffer, pH 7.4, 0.8% NaCl, 0.1% Tween 20, they were incubated in buffer containing the anti–Pvs-ORF239 antibodies for 1.5 hr. After three washes of 5 min each, the grids were floated on buffer containing gold-labeled (10-nm gold particle) goat anti-rabbit antibodies (Auroprobe EMG15; Amersham Life Science)

for 30 min. The grids were washed, dipped vigorously in distilled water, and allowed to dry. The grids were then examined by electron microscopy. To compare results, grids were processed in groups simultaneously. Controls included (1) omission of the primary anti-Pvs-ORF239 antibodies in the described protocol, (2) preabsorption of ORF239 by anti-Pvs-ORF239 antibodies, (3) the rabbit preimmune serum, and (4) primary rabbit anti-MBP antibodies (New England Biolabs).

Fluorescence Microscopy

Floral buds collected from CMS-Sprite, the WPR-3 revertant, and GO8063 were embedded in paraffin as previously described (Berlyn and Mischke, 1976; Johns et al., 1992). Sections 14 μm thick were mounted onto slides with Fink's adhesive (1987). The sections were stained specifically for callose with aniline blue (Jensen, 1962) and observed with fluorescence microscopy.

Cell Wall Preparation, and Gel Blot and Immunocytochemical Analyses

Cell suspension cultures of CMS-Sprite, the WPR-3 revertant, and tobacco (*Nicotiana tabacum* cv W38) were harvested and placed in a 0.75 M NaCl aqueous solution. Cell walls were isolated using a pressure decompression bomb (Carpita 1985; Komalavilas et al., 1991). Briefly, a beaker containing a cell suspension was placed in a stainless steel chamber (Parr Instrument, Moline, IL), and nitrogen (up to 150 atm) was introduced into the chamber. The cell suspension was stirred to facilitate gas diffusion. After equilibrium was reached, the cell suspension was jettisoned into ambient atmospheric pressure. The pressure differential breaks open the cell, and the cytoplasm was released into the solution. The exploded cell solution was then passed through a nylon mesh and washed sequentially with ice-cold solutions of (1) 20 mM NaCl, 20 mM NaOAC, and 50 mM ascorbate, pH 5.5; (2) acetone; (3) 100 mM NaCl; and (4) 200 mM $CaCl_2$, 20 mM NaCl, and 20 mM NaOAc, pH 5.5, to remove all traces of cytoplasm.

Solutions of cell wall preparations were mixed together with 200 μg of the factor Xa cleavage products of the fusion protein. The cleavage products included the uncleaved fusion protein, MBP, and truncated Pvs-ORF239. After incubation for 15 min, the supernatants were collected, and the pelleted cell walls were washed once with 10 mM Tris-HCl, pH 6.6, buffer. Gel electrophoresis and blotting were performed with the supernatant and the wash buffer solution.

The cell walls were used for immunocytological evaluation. Cell walls in suspension were incubated with or without the cleaved fusion protein (MBP, truncated Pvs-ORF239). After several rinses, they were incubated with anti-Pvs-ORF239 antibodies in PBS buffer for 1 hr, rinsed, and incubated with goat anti-rabbit IgG antibodies tagged with gold particles of 15 nm. Silver enhancement of the gold particle with Intense M silver enhancement (Amersham Life Science) was sequential, with three 2-min treatments separated by washes in distilled water. The change of solution was achieved by centrifuging the cell walls for 10 sec at 14,000 rpm (Eppendorf microcentrifuge; Brinkmann Instruments Co., Westbury, NY). Enhancement was monitored by light microscopy. Experimental controls included (1) cell wall preparation minus fusion protein incubation followed by anti-Pvs-ORF239 antibodies, gold-labeled goat anti-rabbit IgG, and silver enhancement; (2) cell wall preparations plus fusion protein incubation but omitting the secondary antibodies prior to silver enhancement; (3) cell wall preparations plus fusion protein incubation but omitting the anti-Pvs-ORF239 antibody incubation; (4) cell wall preparations plus silver enhancement treatment only. To compare data directly, cell wall preparations were run in groups with all the controls.

After incubation of the cell wall preparations with a protein solution containing MBP, truncated Pvs-ORF239, and the fusion protein, the cell walls were centrifuged at 14,000 rpm for 30 sec, and the supernatant was collected for gel analysis.

ACKNOWLEDGMENTS

We thank Dr. Richard Lister for his valuable assistance with ELISA, Dr. Carol Johns for fluorescence microscopy, Dr. John Turek and the staff at the Veterinary Electron Microscopy Facility (Deborah Van Horn and Phyllis Lockard) for support with electron microscopy, and Dr. Nicolas Carpita for assistance in preparation of cell walls from suspension cultures. We also thank Dr. Chris Staiger and Dr. Niels Nielsen for critical review of the manuscript and their exceptionally helpful suggestions. This work was supported by a grant to S.A.M. from the National Science Foundation (Grant No. MCB-9118937). This is journal series No. 14399 from the Indiana Experiment Station.

Received November 7, 1994; accepted January 16, 1995.

REFERENCES

Abad, A.R. (1992). Medium temperature epoxy resin for immunocytochemistry: Quetol 651 with water. Microsc. Res. Tech. **20,** 274–280.

Abad, A.R., Cease, K.R., and Blanchette, R.A. (1988). A rapid technique using epoxy resin Quetol 651 to prepare plant tissues for ultrastructural study. Can. J. Bot. **66,** 667–682.

Albertsen, M.C., and Palmer, R.G. (1979). A comparative light- and electron-microscopic study of microsporogenesis in male sterile (Ms_1) and male fertile soybeans (*Glycine max* (L.) Merr.). Am. J. Bot. **66,** 253–265.

Bassett, M.J., and Shuh, D.M. (1982). Cytoplasmic male sterility in common bean. J. Am. Soc. Hort. Sci. **107,** 791–793.

Berlyn, G.P., and Mischke, J.P. (1976). Fixation and storage. In Botanical Microtechnique and Cytochemistry (Ames, IA: State University Press), pp. 24–34.

Blackmore, S., and Crane, P.R. (1988). The systematic implication of pollen and spore ontogeny. In Ontogeny and Systematics (New York: Columbia University Press), pp. 83–115.

Bradford, M.M. (1976). A rapid and sensitive method for the quantitation of microgram quantities of protein utilizing the principle of protein-dye binding. Anal. Biochem. **72,** 248–254.

Carpita, N.C. (1985). Tensile strength of cell walls of living cells. Plant Physiol. **79,** 485–488.

Chase, C.D. (1994). Expression of CMS unique and flanking mitochondrial DNA sequences in *Phaseolus vulgaris* L. Curr. Genet. **25,** 245–251.

Chase, C.D., and Ortega, V.M. (1992). Organization of ATPA coding and 3′ flanking sequences associated with cytoplasmic male sterility in *Phaseolus vulgaris* L. Curr. Genet. **22,** 147–153.

Chou, P.Y., and Fasman, G.D. (1978). Prediction of the secondary structure of proteins from their amino acid sequence. Adv. Enzymol. **47,** 45–147.

Conley, C.A., and Hanson, M.R. (1994). Tissue-specific protein expression in plant mitochondria. Plant Cell **6,** 85–91.

Devereux, J., Haeberli, P., and Smithies, O. (1984). A comprehensive set of sequence analysis programs for the VAX. Nucleic Acids Res. **12,** 387–395.

Dewey, R.E., Levings, C.S., III, and Timothy, D.H. (1986). Novel recombination in the maize mitochondrial genome produces a unique transcriptional unit in the Texas male-sterile cytoplasm. Cell **44,** 439–449.

Dewey, R.E., Timothy, D.H., and Levings, C.S., III. (1987). A mitochondrial protein associated with cytoplasmic male sterility in the T cytoplasm of maize. Proc. Natl. Acad. Sci. USA **84,** 5374–5378.

Fink, S. (1987). Some new method for affixing sections to glass slides. I. Aqueous adhesives. Stain Technol. **62,** 27–33.

Fry, S.C., Smith, C.R., Renwick, K.F, Martin, D.F., Hodge, S.K., and Matthews, K.J. (1992). Xyloglucan endotransglycosylase, a new wall-loosening enzyme activity from plant. Biochem. J. **282,** 821–828.

Hack, E., Lin, C., Yang, H., and Horner, H.T. (1991). T-URF 13 protein from mitochondria of Texas male-sterile maize (*Zea mays* L.). Plant Physiol. **95,** 861–870.

Hanson, M.R., and Conde, M.F. (1985). Functioning and variation of cytoplasmic genomes: Lessons from cytoplasmic-nuclear interactions affecting male fertility in plants. Int. Rev. Cytol. **94,** 213–267.

He, S., Lyznik, A., and Mackenzie, S. (1995). Pollen fertility restoration by nuclear gene *Fr* in CMS bean: Nuclear-directed alteration of a mitochondrial population. Genetics **139,** 955–962.

Holford, P., Croft, J., and Newbury, H. (1991). Structural studies of microsporogenesis in fertile and male-sterile onions containing the CMS-S cytoplasm. Theor. Appl. Genet. **82,** 745–755.

Horn, R., Kohler, R.H., and Zetsche, K. (1991). A mitochondrial 16 kDa protein is associated with cytoplasmic male sterility in sunflower. Plant Mol. Biol. **17,** 29–36.

Horner, H.T. (1977). A comparative light- and electron-microscopic study of microsporogenesis in male-fertile and cytoplasmic male-sterile sunflower (*Helianthus annuus*). Am. J. Bot. **64,** 745–759.

Horner, H.T., Jr., and Roger, M.A. (1974). A comparative light and electron microscopy study of microsporogenesis in male-fertile and cytoplasmic male-sterile pepper (*Capsicum annuum*). Can. J. Bot. **52,** 435–449.

Huang, J., Struck, F., Matzinger, D.F., and Levings, C.S., III (1994). Flower-enhanced expression of a nuclear-encoded mitochondrial respiratory protein is associated with changes in mitochondrion number. Plant Cell **6,** 439–448.

Izhar, S., and Frankel, R. (1971). Mechanism of male sterility in petunia: The relationship between pH, callase activity in anthers, and the breakdown of microsporogenesis. Theor. Appl. Genet. **41,** 104–108.

Janska, H., and Mackenzie, S.A. (1993). Unusual mitochondrial genome organization in cytoplasmic male sterile common bean and the nature of cytoplasmic reversion to fertility. Genetics **135,** 869–879.

Jensen, W.A. (1962). Preparation of tissue. In Botanical Histochemistry (San Francisco, CA: W.H. Freeman and Co.), pp. 55–144.

Johns, C., Lu, M., Lyznik, A., and Mackenzie, S. (1992). A mitochondrial DNA sequence is associated with abnormal pollen development in cytoplasmic male sterile bean plants. Plant Cell **4,** 435–449.

Johns, C., Nickel, R., McIntosh, L., and Mackenzie, S. (1993). The expression of alternative oxidase and alternative respiratory capacity in cytoplasmic male sterile common bean. Sex. Plant Repro. **6,** 257–265.

Kohler, R.H., Horn, R., Lossl, A., and Zetsche, K. (1991). Cytoplasmic male sterility in sunflower is correlated with the co-transcription of a new open reading frame with the *atpA* gene. Mol. Gen. Genet. **66,** 369–376.

Komalavilas, P., Zhu, J.-K., and Nothnagel, E.A. (1991). Arabinogalactan-proteins from the suspension culture medium and plasma membrane of rose cells. J. Biol. Chem. **266,** 15956–15965.

Konig, B., and Sandermann, H., Jr. (1982). β-D-Galactoside transport in *Escherichia coli:* M_r determination of the transport protein in organic solvent. FEBS Lett. **147,** 31–34.

Krishnasamy, S., and Makaroff, C. (1993). Characterization of the radish mitochondrial *orfB* locus: Possible relationship with male sterility in Ogura radish. Curr. Genet. **24,** 156–163.

Laemmli, U.K. (1970). Cleavage of structural proteins during the assembly of the head of bacteriophage T4. Nature **227,** 680–685.

Laver, H.K., Reynold, S.J., Moneger, F., and Leaver, C.J. (1991). Mitochondrial genome organization and expression associated with cytoplasmic male sterility in sunflower (*Helianthus annus*). Ann. Bot. **64,** 137–148.

Mackenzie, S. (1991). Identification of a sterility-inducing cytoplasm in a fertile line of *Phaseolus vulgaris* L. Genetics **127,** 411–416.

Mackenzie, S., and Bassett, M. (1987). Genetics of restoration in cytoplasmic male sterile *Phaseolus vulgaris* L. Theor. Appl. Genet. **74,** 642–645.

Mackenzie, S.A., and Chase, C.D. (1990). Fertility restoration is associated with loss of a portion of the mitochondrial genome in cytoplasmic male-sterile common bean. Plant Cell **2,** 905–912.

McQueen-Mason, S., Durachko, D.M., and Cosgrove, D.J. (1992). Two endogenous proteins that induce cell wall extension in plants. Plant Cell **4,** 1425–1433.

Moneger, F., Smart, C.J., and Leaver, C.J. (1994). Nuclear restoration of cytoplasmic male sterility in sunflower is associated with tissue-specific regulation of a novel mitochondrial gene. EMBO J. **13,** 8–17.

Nivison, H.T., and Hanson, M.R. (1989). Identification of a mitochondrial protein associated with cytoplasmic male sterility in petunia. Plant Cell **1,** 1121–1130.

Preuss, D., Rhee, S.Y., and Davis, R.W. (1994). Tetrad analysis is possible in *Arabidopsis* with mutation of the *QUARTET* (*QRT*) genes. Science **264,** 1458–1460.

Singh, M., and Brown, G.G. (1991). Suppression of cytoplasmic male sterility by nuclear genes alters expression of a novel mitochondrial gene region. Plant Cell **3,** 1349–1362.

Singh, S.P., White, J.W., and Gutierrez, J.A. (1980). Male sterility in dry beans. Annu. Rep. Bean Improv. Coop. **23,** 55–57.

Smart, C.J., Moneger, F., and Leaver, C.J. (1994). Cell-specific regulation of gene expression in mitochondria during anther development in sunflower. Plant Cell **6,** 811–825.

Towbin, H., Staehelin, T., and Cordon, J. (1979). Electrophoretic transfer of proteins for polyacrylamide gels to nitrocellulose sheets. Proc. Natl. Acad. Sci. USA **76,** 4350–4354.

Warmke, H.E., and Lee, S.-L.J. (1977). Mitochondrial regeneration in Texas cytoplasmic male-sterile corn anthers. J. Hered. **68,** 213–222.

Warmke, H.E., and Overman, M.A. (1972). Cytoplasmic male sterility in sorghum. I. Callose behaviour in fertile and sterile anthers. J. Hered. **63,** 103–108.

Wise, R.P., Pring, D.R., and Gengenbach, B.G. (1987). *Urf13-T* of T cytoplasm maize mitochondria encodes a 13 kD polypeptide. Plant Mol. Biol. **9,** 121–126.

Worrall, D., Hird, D.L., Hodge, R., Paul, W., Draper, J., and Scott, R. (1992). Premature dissolution of the microsporocyte callose wall causes male sterility in transgenic tobacco. Plant Cell **4,** 759–771.

Young, E.G., and Hanson, M.R. (1987). A fused mitochondrial gene associated with cytoplasmic male sterility is developmentally regulated. Cell **50,** 41–49.

Zhang, X.S., and Xi, X.Y. (1991). Ultrastructural studies of microsporogenesis in *Phaseolus vulgaris* L. Acta Bot. Sinica **33,** 267–272.